Retardation effects on collective excitations in correlated superlattices

Kenneth I. Golden
Department of Mathematics and Statistics, University of Vermont, Burlington, Vermont 05401

G. Kalman
Department of Physics, Boston College, Chestnut Hill, Massachusetts 02167

Limin Miao*
Department of Electrical Engineering, University of Vermont, Burlington, Vermont 05405

Robert R. Snapp
Department of Computer Science, University of Vermont, Burlington, Vermont 05405

(Received 10 November 1997; revised manuscript received 5 January 1998)

The authors analyze the effects of electrodynamic retardation on the collective modes in an unmagnetized infinite superlattice modeled as an array of parallel two-dimensional plasma layers embedded in a dielectric substrate. The present work concentrates for the most part on correlated semiconductor superlattices, although the model is equally well suited to metallic superlattices consisting of an alternating array of thin metal layers and thick insulator slabs (e.g., 50 Å Al layers and 500 Å Al_2O_3 slabs). The analysis is based on the transverse magnetic (TM) and transverse electric (TE) dispersion relations recently formulated by the authors in the retarded quasilocalized charge approximation (RQLCA) [K. I. Golden, G. Kalman, L. Miao, and R. R. Snapp, Phys. Rev. B **55**, 16 349 (1997)]. In the nonretarded limit, the QLCA mode structure consists of (i) an isolated in-phase plasmon mode, (ii) a band of gapped plasmons, (iii) an in-phase acoustic shear mode, and (iv) a band of gapped shear modes. This paper presents numerical and approximate analytical solutions of the long-wavelength RQLCA dispersion relations for the collective modes (i)–(iv) all the way down to very small wave numbers where retardation effects can be especially pronounced. Additionally, this work presents insightful approximate analytical formulas for the electromagnetic mode frequencies and gap widths, which add to the literature on the infinite sequences of TM- and TE-polarized electromagnetic bands. Some noteworthy effects that emerge from this study are as follows: (a) The appearance of ultralow frequency shear modes arising from the combined effect of retardation and strong coulomb interactions; the quasilocalization basis of the theory suggests that these modes can propagate when the two-dimensional plasma layers are in a crystalline phase. (b) A negative random-phase approximation shift in the bulk-plasma frequency induced by electrodynamic retardation; this effect can be appreciable in insulator/metal superlattices. [S0163-1829(98)05516-7]

I. INTRODUCTION

In the previous decade a number of investigators[1–5] analyzed the effects of electrodynamic retardation on collective excitations in a variety of infinite superlattice systems. Basing their calculations on the random-phase approximation (RPA) (Refs. 1,4) or on simple RPA-like hydrodynamical models,[2,3,5] these studies do not consider the effects of strong intralayer and interlayer Coulomb interactions. Our own studies,[6] carried out within the quasilocalized charge approximation (QLCA) in the nonretarded ($c\to\infty$) limit, reveal that strong Coulomb interactions profoundly modify the RPA mode structure of unmagnetized semiconductor superlattices. Thus, it remains to be seen how electrodynamic retardation effects add to or extend the QLCA mode structure[6] in correlated superlattices. This is a central theme of the present paper.

The system of interest in this work is the unmagnetized infinite superlattice modeled as an array of two-dimensional (2D) plasma layers embedded in a dielectric substrate. This model is ideally suited to the $GaAs/Al_xGa_{1-x}As$ superlattice and it can also be adapted to metallic superlattices, e.g., Al/Al_2O_3 consisting of alternating thin metallic layers/thick insulator slabs. While metallic superlattices are of some interest in the present work, our main interest will be in correlated semiconductor superlattices, which, in the nonretarded ($c\to\infty$) limit, exhibit an energy gap in the plasmon and shear mode dispersions.[6]

The RPA mode structure of the unmagnetized superlattice consists of (i) an isolated in-phase plasmon mode, (ii) a band of acoustic plasmon modes, (iii) an infinite sequence of transverse magnetic (TM)-polarized (with the magnetic-field vector lying in the superlattice plane) electromagnetic bands,[3,5] and (iv) an infinite sequence of transverse electric (TE)-polarized (with the electric-field vector lying in the superlattice plane) bands.[2,3(b)]

Insofar as the RPA plasmon dispersion is concerned, the effect of electrodynamic retardation is most pronounced at exceedingly small in-plane wave numbers k of the order of $[4\pi n_s e^2/(m^* d c^2)]^{1/2}\equiv \omega_p\sqrt{\varepsilon_s}/c$ (n_s is the areal density of the 2D electron layers, d is the spacing between layers, ω_p is the bulk plasma frequency, ε_s is the substrate dielectric constant). At these k values and extending well into the long-wavelength ($\omega_p\sqrt{\varepsilon_s}/c \ll k \ll 1/d$) domain, the dispersion of

the in-phase plasmon mode was calculated by King-Smith and Inkson[4] to be

$$\omega = kc/\sqrt{\varepsilon_s} \quad \text{for } 0 \leq k \leq \omega_p\sqrt{\varepsilon_s}/c \tag{1.1a}$$

and

$$\omega = \omega_p \quad \text{for } k \geq \omega_p\sqrt{\varepsilon_s}/c, \tag{1.1b}$$

with the RPA acoustic band confined to the $k \geq \omega\sqrt{\varepsilon_s}/c$, $\omega \leq \omega_p$ nonpropagating sector of the ω, k plane; the in-phase plasmon therefore begins as an electromagnetic wave. Its companion in-phase TM electromagnetic mode was calculated to be[4]

$$\omega = \omega_p \quad \text{for } 0 \leq k \leq \omega_p\sqrt{\varepsilon_s}/c \tag{1.2a}$$

and

$$\omega = kc/\sqrt{\varepsilon_s} \quad \text{for } k \geq \omega_p\sqrt{\varepsilon_s}/c, \tag{1.2b}$$

with the TM-polarized electromagnetic bands confined to the $k \leq \omega\sqrt{\varepsilon_s}/c$, $\omega \geq \omega_p$ propagating sector. Equations (1.1) and (1.2) are approximately correct at the RPA level. In the nonretarded limit, we found that the in-phase mode frequency (1.1b) should exhibit a positive RPA frequency shift $(kd)^2\omega_p/24$ arising from higher-order (in kd) terms in the long-wavelength ($kd \ll 1$) expansion of the superlattice form factor $F(k,0) = \sinh(kd)/[\cosh(kd)-1]$.[6(b)] In this paper, enroute to deriving the non-RPA correlational corrections to Eqs. (1.1) and (1.2), we restore the missing nonretarded $(kd)^2\omega_p/24$ RPA correction to Eq. (1.1b). But in so doing, we also discover the existence of a k-independent RPA correction arising from retardation that shifts the bulk-plasma frequency downwards. Admittedly, both RPA corrections are exceedingly small for the semiconductor superlattice in the domain where k is of the order of $\omega_p\sqrt{\varepsilon_s}/c$. Nevertheless, both have the same magnitude there and, as such, should be retained if one is to have a precise mathematical description of the evolution of the in-phase plasmon from $kd=0$ up to kd values in the long-wavelength domain where the nonretarded $O[(kd)^2\omega_p]$ RPA and correlational corrections[6(b)] become dominant.

An equally compelling reason for retaining the retardation correction all the way down to $k=0$ is that the effect appears to be far more pronounced in metallic superlattices. The calculations of Babiker, Constantinou, and Cottam[3(b)] for a metallic superlattice consisting of alternating insulator (1)/metal (2) slabs of comparable thicknesses d_1 and d_2 indicate that retardation brings about an appreciable negative RPA correction in the nonretarded in-phase electromagnetic mode frequency (1.2a). In this paper, we isolate and quantify this effect in insulator/metal superlattices having large d_1/d_2 ratios that can approximate our layered 2D plasma model.

In contrast to the RPA the nonretarded QLCA mode structure of the unmagnetized semiconductor superlattice consists of (i) an isolated in-phase longitudinal plasmon, which, for sufficiently strong interlayer coupling, exhibits crystal-like negative dispersion at long-wavelengths ($kd \ll 1$),[6(b)] (ii) a band of gapped plasmon modes,[6] (iii) an in-phase transverse shear mode that exhibits acoustic-phonon like dispersion at long wavelengths,[6(b)] and (iv) a band of gapped shear modes.[6(b)]

In the present work, we wish to establish a precise mathematical description of the collective mode structure in the domain where both the in-plane and perpendicular wave numbers k and q, are of the order of $\omega_p\sqrt{\varepsilon_s}/c$, that is, where retardation effects are important. In this domain the retarded QLCA (RQLCA) calculations in Secs. II, III, and IV indicate the first vestige of the $k=0$ energy gap in the plasmon frequency and the existence of a new ultralow frequency shear mode stage that arises from the combined effect of strong Coulomb interactions and retardation. The quasilocalization hypothesis underlying the derivation of these modes suggests that they can propagate in a semiconductor superlattice of 2D crystalline plasma layers. According to the calculations of Swierkowski, Neilson, and Szymanski,[7] crystalline plasma layers can form at $r_s = (\pi n_s a_B^{*2})^{1/2} = 25$ for a layer spacing $d = 0.768/(\pi n_s)^{1/2}$ (realizable in a type-I hole superlattice with $n_s = 1.6\times 10^{10}$ cm^{-2} and $d = 343$ Å); a_B^* is the Bohr radius.

The present paper focuses primarily on collective excitations at lower r_s values where the plasma layers are in a liquid phase. The main goal is to analyze the RQLCA dispersion relations for the gapped plasmon and shear modes and to establish approximate analytical formulas for the mode frequencies. Here we are especially interested in the evolution of these modes as k increases from the propagating region $0 \leq k < \omega\sqrt{\varepsilon_s}/c$ to the nonpropagating region $k \geq \omega\sqrt{\varepsilon_s}/c$. Such calculations are necessary preliminaries to the study of the possible radiation mechanisms of oscillations and instabilities in superlattices.

The existence of infinite sequences of TM- and TE-polarized electromagnetic bands separated by gaps arising from the presence of the plasma layers has been reported for a variety of infinite superlattices.[2,3,5] This folding back of the dispersion curves into the first Brillouin zone is a consequence of the translational symmetry of the superlattice. The gaps, which appear at the boundaries of the Brillouin zone, are exceedingly narrow in semiconductor superlattices; however, they are far more pronounced in metallic superlattices. Constantinou and Cottam[3(a)] obtained the TM bands by solving the TM dispersion relation for a superlattice model consisting of an alternating *ABABAB* structure with a 2D electron gas at each interface separating the finite thickness A/B dielectric slabs (modulation-doped GaAs/$Al_xGa_{1-x}As$ superlattice, e.g.). Babiker, Constantinou, and Cottam[3(b)] obtained the TM and TE bands for a metallic superlattice comprised of alternating metal/insulator slabs (Al/Al_2O_3, e.g.) of finite and comparable thicknesses. These investigators and Haupt and Wendler[5] also obtained the TM bands for a metallic superlattice consisting of an alternating metal 1/metal 2 structure (Ag/Al, e.g.) where again the metallic slabs have finite and comparable thicknesses. Our contributions to this topic in the present paper are complementary to the above works in that for the infinite superlattice consisting of 2D electron layers embedded in a dielectric substrate, we establish approximate analytical formulas for the TM- and TE-polarized electromagnetic bands and for the gap widths separating the bands. These oscillation frequency formulas will

therefore be applicable to both semiconductor superlattices and metallic superlattices consisting of alternating thin metal/thick insulator slabs.

The mode frequency calculations of the present paper are based on the RQLCA TM and TE dispersion relations derived by us in Ref. 6(b). The organization of the paper is as follows. In Sec. II we analyze the collective excitations in a homogeneous anisotropic medium model[6(b)] of the correlated superlattice. Such a preliminary model is useful in the vanishing layer separation ($d\to 0$) limit and will be used to provide a physically transparent—albeit simplified and somewhat inconsistent—portrayal of the mode structure and of the polarization of the modes. In Secs. III and IV, we analyze the RQLCA dispersion relations for the superlattice in the long-wavelength ($0\leqslant kd\ll 1$) regime, and we establish approximate analytical mode frequency formulas for (i) the isolated in-phase plasmon and TM electromagnetic modes, (ii) the band of gapped plasmon modes, (iii) the $Q=0$ band of TM-polarized electromagnetic modes (the reciprocal lattice vector $Q=(2\pi/d)s$ or, equivalently, the integer s enumerates the bands), (iv) the in-phase transverse shear mode, (v) the band of gapped shear modes, and (vi) the $Q=0$ band of TE-polarized electromagnetic modes. In Sec. V we establish approximate analytical mode frequency formulas for the $s=1,2,3,\ldots$ TM- and TE-polarized electromagnetic bands, and we calculate the widths of the gaps. Conclusions are drawn in Sec. VI.

II. ANISOTROPIC MEDIUM DESCRIPTION

In general, for a given q value (q is the wave number perpendicular to the lattice planes) both the TM and TE modes split into two independent branches, a high-frequency optical (or, rather, polaritonlike) EM branch and a low-frequency branch. The low-frequency branch of the TM mode can be referred to as the plasmon (P) branch. This latter branch, in the RPA approximation is acoustic, but the acoustic character is destroyed once interlayer correlations are introduced[6] and a $k=0$ gap develops. The low-frequency branch of the TE mode is a shearlike excitation that vanishes in the RPA limit and will be referred to as the S branch; it also develops a gap at $k=0$. Thus, these low-frequency modes are more precisely referred to as ''gapped-plasmon'' (TM) or ''gapped-shear'' (TE) excitations. An exception is the $q=0$ case where the quasiacoustic character ($\omega\to 0$ for $k\to 0$) does survive. The high-frequency EM branches are always on the left of the light line; in contrast, the low-frequency P or S branches exist on both sides of the light line.

In the vanishing layer separation limit, i.e., combined $kd\to 0$, $qd\to 0$ limit, a superlattice can be described as an anisotropic 3D dielectric medium (A3DM). Consider first the TM modes. Solving the Ref. 6(b) A3DM longitudinal dispersion relation (47) with (45) (suitably modified to take account of the correlation-induced electromagnetic effect) and expanding to $O(k^2)$ and $O(q^2)$, one finds the two solutions

$$\omega_+^2=\frac{\omega_p^2}{1+\mathcal{K}}+q^2c_s^2, \tag{2.1a}$$

$$\omega_-^2=k^2c_s^2+q^2c_s^2\mathcal{I}. \tag{2.1b}$$

$$\mathcal{I}(q)=\frac{1}{2}\sum_{m\geqslant 1}[1-\cos(qmd)]|I_{m0}|,$$

$$\mathcal{J}^L(q)=\frac{\delta}{2}\sum_m J^I_{m0}\cos(qmd),$$

$$\mathcal{K}(q)=\frac{\delta}{2}\sum_m K_{m0}\cos(qmd)$$

$$\delta\equiv(\omega_p d/\sqrt{2}c_s)^2,\quad c_s=c/\sqrt{\varepsilon_s}. \tag{2.2}$$

Intralayer (00) and interlayer ($\pm 10,\pm 20,\ldots$) correlational coefficients I_{m0} and J^L_{m0} are defined in Ref. 6(b) in terms of the full hierarchy of superlattice (layer m-layer n) static structure functions $S_{mn}(k)$; the K_{m0} coefficient is similarly defined:

$$K_{|m|0}=\frac{1}{N_e}\sum_{\mathbf{k}'}\frac{1}{k'd}[S_{|m|0}(k')-\delta_{m0}]e^{-k'|m|d}. \tag{2.3}$$

In the $d\to 0$ limit $\mathcal{I}$ is of $O(q^2)$, and thus in the $k=0$ limit the dominant term in ω_-^2 is of $O(q^4)$. In contrast $\mathcal{J}(q)$ and $\mathcal{K}(q)$ assume constant values as $q\to 0$, i.e. $\mathcal{J}^L(0)\approx(\delta/2)\Sigma_m J^L_{|m|0}$, $\mathcal{K}(0)\approx(\delta/2)\Sigma_m K_{|m|0}$. It is of interest to examine the $k\to\infty$ and $q\to\infty$ limits (but keeping in mind that $kd\ll 1$ and $qd\ll 1$ are still satisfied). For $k\to\infty$, $q=0$ one obtains

$$\omega_+^2=k^2c_s^2, \tag{2.4a}$$

$$\omega_-^2=\frac{1}{1+\mathcal{K}}(\omega_p^2+k^2c_s^2\mathcal{J}^L), \tag{2.4b}$$

while in the $q\to\infty$, $k=0$ limit one has

$$\omega_+^2=q^2c_s^2+\omega_p^2, \tag{2.5a}$$

$$\omega_-^2=\mathcal{I}(q)\omega_p^2\approx\frac{1}{4}\omega_p^2q^2d^2\sum_{m\geqslant 1}m^2|I_{m0}|. \tag{2.5b}$$

Thus, the picture that emerges from this treatment comprises two modes with complementary behaviors. The eigenmodes are polarized in the kq plane. But it should be noted that, in general, neither of them is polarized in the $\mathbf{k}=\hat{e}_x k$ or $\mathbf{q}=\hat{e}_z q$ directions. The polarizations also change along the two branches as a function of $\mathbf{k}$. In the absence of correlations the P branch (ω_-) starts out along the light line as a transverse wave propagating along $\mathbf{k}$ (since it is polarized along z, it is unaffected by the plasma frequency) and ends up as a bulk plasmon (with longitudinal polarization along x) at ω_p. On the other hand, the EM branch (ω_+) also starts out as a transverse wave propagating along q (and polarized along x and thus affected by the plasma frequency) and ends up along the light line as an EM wave polarized along z. The principal modification due to correlations is manifested through the second term in Eq. (2.1b): it represents a correlation maintained shear wave propagating along q with the peculiar $\omega\sim q^2$ dispersion. This depression of the normally acoustic shear mode dispersion is an electromagnetic effect and an identical behavior has already been demonstrated in

strongly coupled 3D plasmas.[8] Increasing q (over ω/c) brings the shear mode into the linear domain [cf. (2.5)].[6(b)]

Further correlational effects are associated with the $k^2c_s^2\mathcal{J}^L$ and $\omega_p^2/(1+\mathcal{K})$ terms in Eqs. (2.1) and (2.4). The former represent the negative plasmon dispersion (note that $\mathcal{J}^L<0$) induced by correlations: this again is well known in the 3D situation. The latter generates a positive shift ($\mathcal{K}<0$) of the plasmon frequency due to a combined effect of the correlations and transverse interaction: this effect was discussed in Refs. 8 and 9.

We turn next to the A3DM description of the TE modes. These modes are isotropic in the sense that the correlation-independent terms depend on (q^2+k^2) only. For small q and k the two modes are

$$\omega_+^2=\frac{\omega_p^2}{1+\mathcal{K}}+(q^2+k^2)c_s^2, \tag{2.6a}$$

$$\omega_-^2=(k^2+q^2)c_s^2\left(\mathcal{I}(q)+\mathcal{J}^T\frac{k^2c_s^2}{\omega_p^2}\right). \tag{2.6b}$$

The high k ($q=0$) and high q ($k=0$) limits are simply

$$\omega_+^2=k^2c_s^2+\omega_p^2, \tag{2.7a}$$

$$\omega_-^2=\frac{1}{1+\mathcal{K}}\,\mathcal{J}^Tk^2c_s^2, \tag{2.7b}$$

and

$$\omega_+^2=q^2c_s^2+\omega_p^2, \tag{2.8a}$$

$$\omega_-^2=\mathcal{I}(q)\omega_p^2, \tag{2.8b}$$

where $\mathcal{J}^T=\Sigma_m J^T_{|m|0}$ with $J^T_{|m|0}$ given by Eqs. (30) and (33) of Ref. 6(b). In contrast to the TM modes, the polarization is always fixed along the y axis. The ω_+ EM branch is similar to that in a (3D) plasma. The ω_- branch is a gapped shear excitation with the typical $\omega^2\sim q^4$ type dispersion.

III. SUPERLATTICE TM MODES

The A3DM misses noncorrelational effects, which are caused by finite layer separation. Foremost amongst these in the nonretarded limit is the acoustic plasmon.[10] In general, a rigorous analysis requires the analysis of the superlattice longitudinal dispersion relation (16) of Ref. 6(b) [combined with RQLCA Eq. (15) of that same reference] to which we now turn. Concentrating on the long-wavelength ($kd\ll 1$) regime of interest in the present work, our task can be reduced to finding solutions for $\kappa^2\equiv(\omega/c_s)^2-k^2$ of the small k dispersion relation

$$\begin{aligned}&\kappa^2d^2\left(1+\frac{\delta}{2}\sum_m K_{|m|0}\cos(qmd)\right)\\&\quad+k^2d^2\left(1+\frac{\delta}{2}\sum_m (K_{|m|0}-J^L_{|m|0})\cos(qmd)\right)\\&\quad=-\frac{\delta\kappa d\,\sin\,\kappa d}{\cos\,\kappa d-\cos\,qd}+\delta\sum_{m\geqslant 1}[1-\cos(qmd)]|I_{m0}|.\end{aligned} \tag{3.1}$$

Solutions $\kappa^2=\kappa_-^2<0$ correspond to propagation along the in-plane wave vector $\mathbf{k}$ with exponential decay of the perturbed field quantities in the z direction. Solutions $\kappa^2=\kappa_+^2>0$ correspond to oblique propagation along the wave vector $\mathbf{K}_+=\mathbf{k}+\hat{\mathbf{e}}_z\kappa_+$ which lies in the xz plane if one takes $\mathbf{k}=\hat{\mathbf{e}}_xk$. The analysis consists in solving Eq. (3.1) for κd as a function of kd while holding the mode parameter qd fixed in the two intervals $0\leqslant(qd)^2\ll 2\delta$ and $2\delta\ll(qd)^2\leqslant\pi^2$. The quantity $2\delta\equiv(\omega_pd/c_s)^2$ serves as a convenient reference point for organizing the calculations. Unless otherwise stipulated, we assume that $\delta\ll 1$, which is always the case for semiconductor superlattices.

A. In-phase modes

Beginning with the in-phase ($qd=0$) modes, we seek solutions to Eq. (3.1) such that $\kappa^2d^2\ll 1$, consistent with the assumed smallness of δ, qd, and kd. Using a straightforward method of successive approximations with the trigonometric functions replaced by their small-argument expansions, one obtains two solutions $\kappa_\pm$: the $(+)$ solution refers to the in-phase TM EM branch and the $(-)$ solution to the in-phase plasmon. The corresponding frequencies are calculated to be:

$$\omega_+^2(k,0)=\begin{cases}\dfrac{\omega_p^2}{1+\dfrac{\delta}{6}+\dfrac{\delta}{2}\displaystyle\sum_m K_{|m|0}}\left[1+k^2d^2\left(\frac{1}{12}+\frac{1}{4}\displaystyle\sum_m J^L_{|m|0}\right)\right] & \text{for } 0\leqslant(kd)^2\leqslant 2\delta^* \quad (3.2a)\\ (kc_s)^2 & \text{for } (kd)^2\geqslant 2\delta^* \quad (3.2b)\end{cases}$$

$$\omega_-^2(k,0)=\begin{cases}(kc_s)^2 & \text{for } 0\leqslant(kd)^2\leqslant 2\delta^* \quad (3.3a)\\ \dfrac{\omega_p^2}{1+\dfrac{\delta}{6}+\dfrac{\delta}{2}\displaystyle\sum_m K_{|m|0}}\left[1+k^2d^2\left(\frac{1}{12}+\frac{1}{4}\displaystyle\sum_m J^L_{|m|0}\right)\right] & \text{for } (kd)^2\geqslant 2\delta^* \quad (3.3b)\end{cases}$$

$$\delta^* = \frac{\delta}{1 + \frac{\delta}{2} \sum_m (K_{|m|0} - J^L_{|m|0})}. \tag{3.4}$$

Formulas (3.2b) and (3.3b) are the superlattice counterparts of A3DM Eqs. (2.4). The plasmon frequency in (3.3b) exhibits the positive RPA dispersion $(kd)^2/24$ and the negative correlation-induced Coulomb dispersion $[-(k^2d^2/8)|\Sigma_m J^L_{|m|0}|]$ discussed above and in Ref. 6(b). Retardation effects show up in Eq. (3.2) as the negative RPA and positive correlational shifts $-\delta\omega_p/12$ and $+(\delta\omega_p/4)|\Sigma_m K_{|m|0}|$ in the plasma frequency. For the semiconductor superlattice model of this paper (an array of 2D electron liquid monolayers embedded in a dielectric substrate), these shifts are exceedingly small in the weak coupling regime ($\delta = 1.64\times10^{-4}$ for GaAs/Al_xGa_{1-x}As with $n_s = 7.3\times10^{11}$ cm^{-2}, $d = 890$ Å, $m^* = .07m_s$, $\varepsilon_s = 13.1$) and even smaller in the strong-coupling regime ($\delta = 1.62\times10^{-6}$ for $n_s = 1.3\times10^{10}$ cm^{-2}, $d = 500$ Å). Nevertheless, the $O(\delta)$ corrections are retained in Eq. (3.3b) [and consequently in Eq. (3.2a)] in order to present a precise analytical description of the evolution of the in-phase plasmon as kd increases from $\sqrt{2\delta^*}$ [where the $O(\delta)$ and $O(k^2d^2)$ corrections are comparable] to values well beyond $\sqrt{2\delta^*}$ where the $O(k^2d^2)$ dispersion eventually dominates. The next paragraph digresses somewhat to present an equally compelling reason for retaining the $O(\delta)$ corrections in Eq. (3.2a) and in Eq. (3.5) below.

Retardation effects become more pronounced with increasing d and n_s: thus, they are expected to be of more significance in metallic superlattices. This has already been pointed out by Babiker, Constantinou, and Cottam (BCC)[3(b)] (but without giving a mathematical description of the effect) in relation to metallic superlattices modeled as alternating insulator (1)/metal (2) slabs of comparable finite thicknesses d_1 and d_2. This is also the case when the metallic layers are thin compared with the insulator layers so that the metallic superlattice can be modelled as an array of 2D plasma layers embedded in an insulator substrate. Consider first the situation where the slab thicknesses are comparable. In the nonretarded ($c\to\infty$) limit, the BCC formula for the in-phase $kd = 0$ plasmon frequency $\omega_\infty = \omega_{p2}[1 + \varepsilon_1(d_1/d_2)]^{-1/2}$ can be readily derived from the BCC alternating slab dispersion relation [Eq. (5.1) in Ref. 3(b)]. Using the approximate numerical values $\omega_{p2} = 15$ eV, $\epsilon_1 = 3$, $d_1 = 100$ Å, $d_2 = 50$ Å quoted from Babiker, Constantinou, and Cottam[3(b)] for an Al_2O_3/Al superlattice, we calculate $\omega_+(0,0)|_{\rm BCC} \approx 0.987\omega_\infty$ from the BCC retarded dispersion relation [Eq. (4.2) in Ref. 3(b)], i.e., a negative RPA shift of 1.3%. This shift becomes more pronounced at the higher d_1/d_2 ratios which begin to approximate the layered 2D electron liquid model of this paper; for example, with $d_1 = 500$ Å $\gg d_2 = 50$ Å [see, for example, Jin and Ketterson[11]], we calculate $\omega_\infty = 0.180\omega_{p2}$ and $\omega_+(0,0)|_{\rm BCC} = 0.942\omega_\infty$ giving a negative RPA shift of 5.8%. This compares quite well with the RPA shift calculated from Eq. (3.2a): with the bulk-plasma frequency given as $\omega_p = \omega_{p2}[d_2/(\varepsilon_1 d_1)]^{1/2} = 0.182\omega_{p2} \approx \omega_\infty$ and $\delta = \omega_{p2}^2 d_2 d_1/(2c^2) = 0.721$, we obtain $\omega_+(0,0) = 0.945\omega_p$, giving a 5.5% shift. Even better agreement is obtained using the parent TM dispersion relation (3.1) instead of Eq. (3.2a): we calculate a 5.7% negative RPA shift. This is not surprising considering that the derivation of Eq. (3.2a) from Eq. (3.1) assumes $\delta \ll 1$, which is no longer the case here.

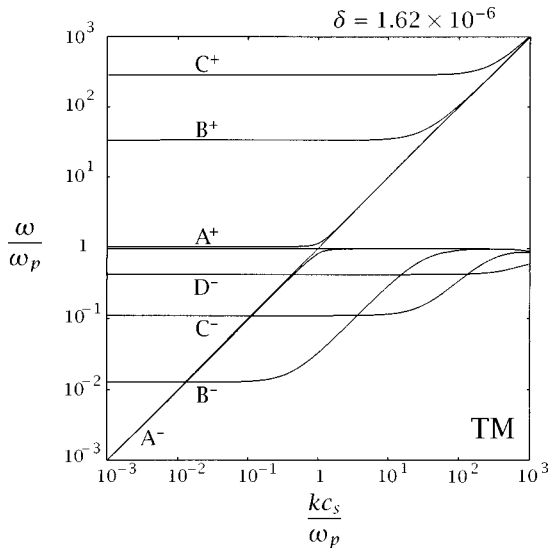

FIG. 1. TM plasmon (P) and electromagnetic (EM) dispersion curves calculated from Eq. (3.1) for a strongly correlated GaAs/AlGaAs superlattice ($\delta = 1.62\times10^{-6}$ for $n_s = 1.3\times10^{10}$ cm^{-2} and $d = 500$ Å). The EM (+) and P (−) modes are labeled by qd values: $A_\pm(qd = 6\times10^{-4})$, $B_\pm(qd = 6\times10^{-2})$, $C_\pm(qd = \pi/6)$, $D_-(qd = \pi)$.

For the Al_2O_3/Al superlattice with $\omega_{p2} = 15$ eV, the $r_s = 2.8$ value suggests that the positive shift arising from the K_{00} intralayer coefficient might be significant (interlayer correlational effects are insignificant in virtue of the smallness of the coupling parameter $r_s a/d_1 \approx 0.008$ for $d_1 = 500$ Å). Our $K_{00} \approx -0.003$ estimate, in fact, indicates that the positive intralayer correlational shift is swamped by the negative RPA shift. Thus, for metallic superlattices modeled as alternating insulator (1)/metal (2) slabs with large d_1/d_2 ratios, the $kd = 0$ in-phase TM mode frequency is reasonably well described by the $kd = 0$ RPA limit of Eq. (3.2a) and, consequently, by the RPA limit of Eq. (3.5) below.

B. $0 < (qd)^2 \ll 2\delta$

Returning to the semiconductor superlattice, we extend now the calculation of the mode frequencies to nonzero qd values in the very narrow interval $0 < (qd)^2 \ll 2\delta$. The analysis is facilitated by dividing the problem into the two kd subintervals $0 \leqslant (kd)^2 \ll 2\delta$ and $2\delta \ll (kd)^2 \ll 1$. Thus the ω_+ EM mode is represented by Eq. (3.2) at $qd = 0$, and ω_- is now the ''gapped'' ($\omega \neq 0$ for $k = 0$) P mode.

For kd values in the very narrow interval $0 \leqslant (kd)^2 \ll 2\delta$, the EM branch dispersion is portrayed by Fig. 1, curve A_+

$$\omega_+^2(k,q)=\frac{\omega_p^2}{1+\frac{\delta}{6}+\frac{\delta}{2}\sum_m K_{|m|0}}+q^2c_s^2 + \omega_p^2k^2d^2\left(\frac{1}{12}+\frac{1}{4}\sum_m J^L_{|m|0}\right) + \frac{q^2k^2c_s^4}{\omega_p^2}+O(\omega_p^2\delta^2). \tag{3.5}$$

The P branch (Fig. 1, curve A_-)

$$\omega_-^2(k,q)=k^2c_s^2\left(1-\frac{q^2c_s^2}{\omega_p^2}-\frac{q^2d^2}{4}\sum_m (K_{|m|0}-J^L_{|m|0})\right) + \frac{q^4c_s^2d^2}{4}\sum_{m\geqslant 1} m^2|I_{m0}| \tag{3.6}$$

also exhibits electromagneticlike dispersion. Formulas (3.5) and (3.6) can be compared with A3DM formulas (2.1). These latter are calculated with the assumption that $d\to 0$ and $k^2c^2\ll\omega^2$. Equations (3.5) and (3.6), on the other hand, are the outcome of a formal expansion in kd and qd.

Wave number q having lost its role as the third component of the wave vector, the last term in Eq. (3.6) should be regarded as a ''gap.'' The polarization of this mode has already been discussed. The quasilocalization hypothesis underlying the derivation of Eq. (3.6) suggests that this low-frequency mode exists as well when the lattice planes are in a 2D Wigner crystal phase.[7] When the lattice planes are not crystalline, the survival of this initial stage of the gap in Eq. (3.6) is, in fact, unlikely since in a 2D Coulomb liquid phase the migration-diffusion time τ_D of the particles away from their instantaneous positions is far too short compared with the mode oscillation time to justify the RQLCA basis of Eq. (3.6) [Ref. 6(b)]. This suggests that when the lattice planes are in the liquid phase, the correlational terms in Eq. (3.6) can be discarded, leaving only RPA plasmon dispersion,[4] which is always confined to the lower-right quadrant bounded by the $qd=0$ P branch and the kd axis.

As $(kd)^2$ increases well beyond 2δ to the point where it is in the interval $2\delta\ll(kd)^2\ll 1$, the A_- branch evolves eventually into the nonretarded longitudinal bulk plasmon reported [as Eq. (40)] in Ref. 6(b). This quasistatic behavior is characterized by an acoustic ($\omega\propto q$) gap, which in the quasistatic limit arises at $k=0$ [see Eq. (39) of Ref. 6(b)]. In the present fully retarded description the acoustic gap is slightly shifted and is reached at the light line:

$$\omega^2(k=\omega/c_s)=\frac{\omega_p^2}{4}\,q^2d^2\,\frac{\sum_{m\geqslant 1} m^2|I_{m0}|}{1+\frac{\delta}{2}\sum_m (K_{|m|0}-J^L_{|m|0})} \tag{3.7}$$

as it can be easily verified directly from Eq. (3.1). The gap is followed by the quasiacoustic plasmon dispersion portrayed by Eqs. (41) and (42) of Ref. 6(b). This development is not portrayed correctly by the A3DM because of the missing acoustic portion of the dispersion.

The companion (A_+) EM branch dispersion[4]

$$\omega_+^2(\mathbf{k},q)=(k^2+q^2)c_s^2+\omega_p^2\,\frac{q^2}{k^2} \tag{3.8}$$

asymptotically approaches the light line: this can be compared with ω_+^2 in Eq. (2.4). Correlational terms are not displayed in Eq. (3.8) since they would eventually show up as very high-order undetectable contributions.

C. $2\delta\ll(qd)^2\leqslant\pi^2$

We consider next the long-wavelength modes for qd values in the far wider interval $2\delta\ll(qd)^2\leqslant\pi^2$.

Addressing first the EM branch, one again seeks solutions to Eq. (3.1) such that (i) $|\kappa d|\ll 1$ for $|qd|\ll 1$ and (ii) $\kappa d=qd+\varepsilon$ for qd finite; for (ii) the task consists in calculating the small positive correction $\varepsilon\ll|qd|$. After some algebra involving successive approximations, one obtains the same result for (i) and (ii) above (Fig. 1, curves B_+,C_+):

$$\omega_+^2(k,q)=(k^2+q^2)c_s^2+\omega_p^2\,\frac{q^2}{q^2+k^2}, \tag{3.9}$$

valid for $2\delta\ll(qd)^2<\pi^2$ and over the entire long-wavelength interval $0\leqslant(kd)^2\ll 1$. A3DM formula (2.5a) is the $k=0$ counterpart of Eq. (3.9). The mode frequency (3.9) can also be derived from the King-Smith-Inkson RPA Eq. (3.10);[4] our result, however, is not restricted to $|qd|\ll 1$. The calculation of the EM frequency at the edge of the Brillouin zone $|qd|=\pi$ calls for a separate successive approximation treatment that yields

$$\omega_+^2\left(k,\pm\frac{\pi}{d}\right)=\left(\frac{\pi^2}{d^2}+k^2\right)c_s^2. \tag{3.10}$$

Addressing next the P branch, we wish to calculate small-kd solutions of Eq. (3.1) first for qd values in the more restricted interval $2\delta\ll(qd)^2\ll 1$. Again, using the method of successive approximations, one arrives at the gapped-plasmon solution (Fig. 1, curve B_-)

$$\omega_-^2(k,q)=\omega_p^2\left[\left(\frac{q^2d^2}{4}-\frac{\delta}{2}\right)\sum_{m\geqslant 1} m^2|I_{m0}|+\frac{k^2}{q^2}\right] \tag{3.11}$$

for $(kd)^2\ll 2\delta\ll(qd)^2\ll 1$. The nonretarded acoustic (in q) shear mode reported [as Eq. (39)] in Ref. 6(b) and in the present work as A3DM Eq. (2.5b) is readily recovered from Eq. (3.11) by first setting $k=0$ and then going to the nonretarded limit $\delta=0$. From the discussion below Eq. (3.6), the quasilocalization hypothesis underlying the derivation of Eq. (3.11) requires $\omega\tau_D>1$. Thus, there exists a critical q min below which the validity of the QLCA hypothesis becomes questionable.

When kd is further increased along B_- to values in the interval $2\delta\ll(qd)^2\ll(kd)^2\ll 1$, successive approximation calculations result in the bulk mode dispersion

$$\omega_-^2(k,q)=\omega_p^2\left[1+k^2d^2\left(\frac{1}{12}+\frac{1}{4}\sum_m J^L_{|m|0}\right)-\frac{q^2}{k^2}\right]. \tag{3.12}$$

For finite $|qd|$ values up to the edge of the Brillouin zone, the effect of retardation on plasmon dispersion becomes even more insignificant for kd in the interval $2\delta \ll (kd)^2 \ll 1$. The plasmon mode is therefore quite accurately portrayed by the nonretarded Eq. (36) of Ref. 6(b) and in Fig. 1 as curve C_- (well beyond the elbow). At exceedingly small wave numbers $(kd)^2 \ll 2\delta$, taking account of electrodynamic retardation would merely add an $O(\delta)$ correction to the nonretarded $k=0$ gapped band reported [as Eq. (38)] in Ref. 6(b).

There is no merging of the $k \to 0$ portion of the gapped plasmon modes into the pair excitation continuum, thus precluding the possibility of Landau damping of these modes.

IV. SUPERLATTICE TE MODES

We turn next to the analysis of the superlattice transverse dispersion relation (17) [combined with RQLCA Eq. (15)] of Ref. 6(b). At long wavelengths the TE dispersion relation analogous to Eq. (3.1) is given by

$$\kappa^2 d^2 \left(1 + \frac{\delta \sin \kappa d}{\kappa d(\cos \kappa d - \cos qd)} + \frac{\delta}{2} \sum_m K_{|m|0} \cos(qmd) \right) + k^2 d^2 \left(1 + \frac{\delta \sin \kappa d}{\kappa d(\cos \kappa d - \cos qd)} + \frac{\delta}{2} \sum_m (K_{|m|0} - J^T_{|m|0}) \cos(qmd) \right) = \delta \sum_{m \geq 1} [1 - \cos(qmd)] |I_{m0}|. \quad (4.1)$$

Following the analytical procedure of Sec. III our task consists in determining solutions $\kappa_\pm d$ of Eq. (4.1); here the $(+)$ solutions refer to the EM branch and the $(-)$ solutions to the S branch. The problem then consists in solving Eq. (4.1) for κd as a function of kd for fixed qd values in each of the two intervals $0 \leq (qd)^2 \ll 2\delta$ and $2\delta \ll (qd)^2 \leq \pi^2$, where again, we assume $\delta \ll 1$. The in-phase $q=0$ limit plays no special role for the TE mode and therefore, it will not be afforded a special treatment.

We consider first the EM branch. Beginning with kd values in the very narrow interval $0 \leq (kd)^2 \ll 2\delta$, we solve the dispersion relation (4.1) by successive approximation to obtain

$$\omega_+^2(k,q) = \frac{\omega_p^2}{1 + \frac{\delta}{6} + \frac{\delta}{2} \sum_m K_{|m|0}} + (k^2 + q^2) c_s^2. \quad (4.2)$$

The dispersion is shown in Fig. 2 as curves A_+ (for $qd=0$) and B_+ [for $0 < (qd)^2 \ll 2\delta$]. Equation (4.2) is the superlattice counterpart of A3DM Eq. (2.6a). At $qd=0=kd$, TE and TM mode frequencies (4.2) and (3.2a) are identical. If kd is increased along curve A_+ (or B_+) (while holding qd fixed) to some value in the wider interval $0 \leq (qd)^2 \ll 2\delta \ll (kd)^2 \ll 1$, the mode frequency (4.2) evolves into the RPA dispersion $\omega_+^2 = \omega_p^2 + (k^2+q^2)c_s^2$ reported by King-Smith and Inkson.[4]

For qd in the far wider interval $2\delta \ll (qd)^2 < \pi^2$, our successive approximation calculation again yields the above

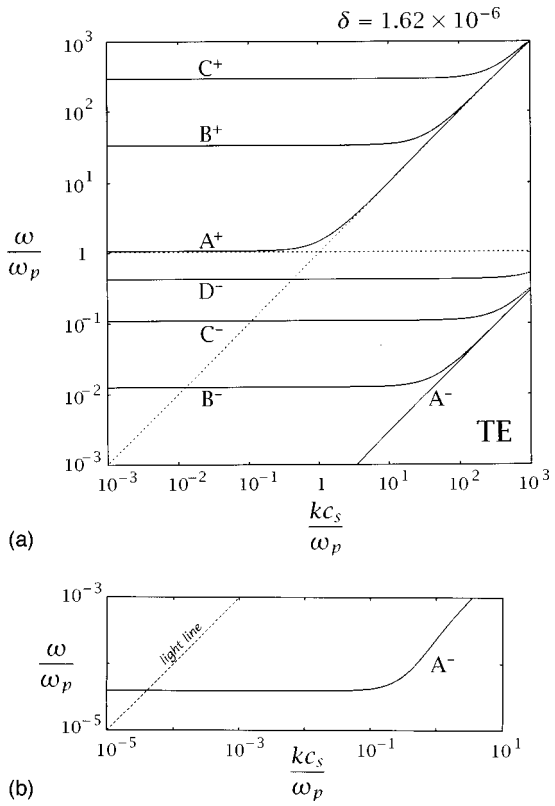

FIG. 2. TE shear (S) and electromagnetic (EM) dispersion curves calculated from Eq. (4.1) for the superlattice of Fig. 1 with the same qd values. The dotted line $\omega/\omega_p \approx 1$ and $\omega = kc_s$ light line corresponding to the $qd=0$ TM mode is shown as a reference curve. 2(b) is a magnified picture of the A_- S curve.

King-Smith and Inkson TE mode (Fig. 2, curve C_+) valid over the entire long-wavelength interval $0 \leq (kd)^2 \ll 1$. This mode is the superlattice counterpart of A3DM Eqs. (2.7a) and (2.8a). Similarly to the TM analysis, the calculation of the TE mode frequency at $|qd| = \pi$ calls for a separate successive approximation treatment, which results in the mode frequency (3.10). Our analysis therefore extends the King-Smith and Inkson small-qd TE electromagnetic mode calculation[4] into the finite-qd domain right up to the edge of the Brillouin zone.

We consider next the long-wavelength dispersion of the S branch. Beginning with the in-phase $(qd=0)$ mode, we solve Eq. (4.1) to obtain (Fig. 2, curve A_-)

$$\omega_-^2(k,0) = \frac{k^4 c_s^2 d^2}{4} \sum_m J^T_{|m|0}, \quad (4.3)$$

for $(kd)^2 \ll 2\delta$ and

$$\omega_-^2(k,0) = \omega_p^2 \left(\frac{k^2 d^2}{4} - \frac{\delta}{2} \right) \sum_m J^T_{|m|0} \quad (4.4)$$

for $2\delta \ll (kd)^2 \ll 1$ (again, Fig. 2, curve A_-). Equation (4.3) is the $q=0$ superlattice counterpart to A3DM formula (2.6b). Equation (4.4) corresponds to A3DM Eq. (2.7b). The denominator factor $(1 + (\delta/6) + (\delta/2)\Sigma_m K_{|m|0})$ corresponding to $(1+\mathcal{K})$ has been left out of Eq. (4.4) because it is a higher-order (in δ) correction [as it is in Eq. (2.7b)]. Equation (4.4) also applies to qd values in the narrow interval

$0 \leqslant (qd)^2 \ll 2\delta$ (Fig. 2, curve B_-). The quasilocalization hypothesis underlying the derivation of Eq. (4.3) suggests that such a mode can propagate (along $\mathbf{k}$) in a superlattice if its lattice planes are in a crystalline phase. In an earlier work, Golden and co-workers[8] reported the emergence of a similarly structured ($\omega \propto k_{3D}^2$) shear mode in the strongly coupled classical 3D OCP again suggesting the existence of the quadratic stage in the 3D OCP crystal.

As to the viability of the ultralow frequency mode (4.3) in the layered 2D electron liquid phase, the discussion below Eq. (3.6) and in Ref. 8 indicates that this mode, like its 3D OCP counterpart, cannot be maintained by particle correlations in a normal strongly coupled Coulomb liquid.

On the other hand, the acoustic shear excitation (4.4) can be maintained by particle correlations in a Coulomb liquid so long as the migration-diffusion time τ_D is longer than the mode oscillation time, i.e., $\omega\tau_D > 1$ (corresponding to k greater than some $k_{\min}$; see discussion in Ref. 8); the acoustic shear wave (4.4) is therefore expected to propagate when the 2D electron layers are in a strongly correlated Coulomb liquid phase. But then there is still the separate question of decay of this mode by pair excitations (Landau damping) to consider. To approximately determine the critical r_s where the mode merges with the pair continuum, it suffices to compare the Fermi velocity with the phase velocity of a shear wave propagating in a 2D electron liquid monolayer.[12] The latter depends on the correlation energy, which is reasonably well approximated by the Tanatar-Ceperley[13] (Monte Carlo-based) formula for the ground-state energy of the 2D crystal phase. Our calculation indicates that at r_s values below 17.5, the in-phase acoustic shear mode lies inside the pair continuum and is, therefore, heavily Landau damped. Thus, in-phase shear waves can propagate only if the intralayer coupling is sufficiently high and then only at wave numbers $k > k_{\min} \gg \sqrt{2\delta}/d$.

For $0 \leqslant (qd)^2 \ll 2\delta$ and $0 \leqslant (kd)^2 \ll 2\delta$, our analysis of the TE dispersion relation (4.1) results in the ultralow frequency gapped S mode

$$\omega_-^2(k,q) = \frac{1}{4}(k^2+q^2)c_s^2\left(q^2d^2\sum_{m\geqslant 1}|I_{m0}| + k^2d^2\sum_m J^T_{|m|0}\right). \tag{4.5}$$

Equation (4.5) is the full superlattice counterpart of A3DM Eq. (2.6b). Again, this stage is expected to be viable in a semiconductor superlattice array of 2D crystalline layers.

For qd values in the much wider interval $2\delta \ll (qd)^2 \ll 1$, our calculations yield (Fig. 2, curve C_-)

$$\omega_-^2(k,q) = \frac{\omega_p^2}{4}\left(q^2d^2\sum_{m\geqslant 1}|I_{m0}| + k^2d^2\sum_m J^T_{|m|0}\right) \times\left[1 - \frac{2\delta}{(k^2+q^2)d^2}\right]. \tag{4.6}$$

valid over the long-wavelength interval $2\delta \ll k^2d^2 \ll 1$. In the $kd = 0$ limit, the gap values obtained from Eqs. (4.5) and (4.6) are identical—as they should be—to their respective plasmon counterpart Eqs. (3.6) and (3.11). (The distinction between the S and P modes is meaningless at $kd = 0$.)

For finite $|qd|$ values up to π and for $0 \leqslant (kd)^2 \ll 2\delta$, our analysis of Eq. (4.1) results in the nonretarded gapped shear excitation (38) of Ref. 6(b) with an additional $O(\delta)$ correction term arising from retardation. In the much wider interval $2\delta \ll (kd)^2 \ll 1$, we recover the nonretarded shear mode dispersion (37) of Ref. 6(b) with the same additional $O(\delta)$ correction attached to the gapped term.

Shear waves with phase velocities below the Fermi velocity would be heavily Landau damped were it not for the energy gap; instead, only the lower energy portion of the shear band penetrates the pair continuum for some $k > k^*$ in the long-wavelength domain.[6(b)] For phase velocities above the Fermi velocity, i.e., for $r_s > 17.5$, we have shown that the in-phase ($qd = 0$) mode lies above the pair continuum. Hence all of the higher lying gapped shear excitations also lie above the continuum and, consequently, escape decay by pair excitations (Landau damping). One can therefore conclude that Landau damping should not seriously affect the long-wavelength shear wave propagation when the 2D electron layers are in correlated liquid phase.

V. HIGHER-FREQUENCY ELECTROMAGNETIC BANDS

In addition to the fundamental TM and TE electromagnetic modes portrayed by Eqs. (3.2a), (3.5), (3.8)–(3.10) and (4.2), the superlattice exhibits an infinite sequence of higher-lying TM- and TE EM bands separated by band gaps (not to be confused with the correlational $k = 0$ gaps), which arise from the presence of the plasma layers. Each band is characterized by the value of the reciprocal lattice vector $Q = 2\pi s/d$, where s is a positive integer that labels the band; the fundamental TM and TE EM branches (analyzed in the previous sections) are assigned the label $s = 0$. Moreover, each $s \geqslant 1$ band consists of a lower (l) subband and an upper (u) subband, which appear as zig-zag lines in the ω-q plane for a fixed value of the in-plane wave number k (Figs. 3 and 4); this folding back of the dispersion curves is due to the translational symmetry of the superlattice.

The infinite higher-lying gapped bands have been reported by a number of investigators[3,5] for a variety of superlattice configurations described in the Introduction. The calculations that follow are complementary to the studies of Constantinou and Cottam[3] and Haupt and Wendler[5] in that they provide approximate analytical formulas for the TM and TE electromagnetic bands in an infinite superlattice array of 2D plasma layers embedded in a dielectric substrate. These formulas will therefore be applicable both to semiconductor superlattices and to metallic superlattices modelled as an array of 2D metallic layers embedded in an insulating substrate.

In calculating the mode frequencies from TM Eq. (3.1) and TE Eq. (4.1), one can show that the correlational contributions are even more insignificant for the higher lying electromagnetic bands. Thus, it suffices to solve Eqs. (3.1) and (4.1) with the correlational coefficients $I_{|m|0}, K_{m|0}, J^{L,T}_{|m|0}$ set equal to zero. The subband frequencies can be readily calculated by assuming solutions of the form $\kappa d = (Q \pm q)d + \varepsilon$ where ε is a small quantity to be determined by substitution into the RPA limit of Eqs. (3.6) and (4.4). After some algebra one obtains

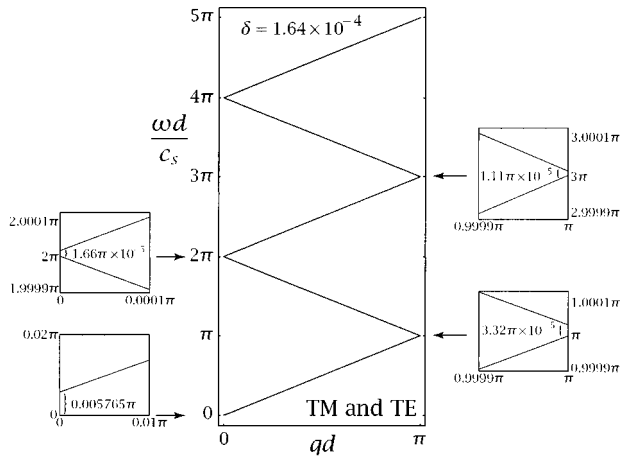

FIG. 3. Common TM and TE frequency at $kd=0$ vs qd in the first Brillouin zone for the $s=0,1,2$, electromagnetic bands in an uncorrelated GaAs/Al_xGa_{1-x}As superlattice ($\delta=1.64\times10^{-4}$ for $n_s=7.3\times10^{11}$ cm^{-2} and $d=890$ Å) calculated from Eq. (3.1) or (4.1) at $kd=0$.

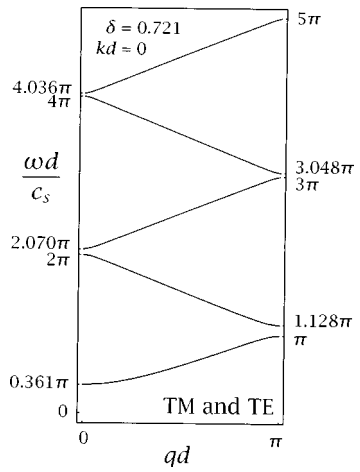

FIG. 4. Common TM and TE frequency at $kd=0$ vs qd in the first Brillouin zone for the $s=0,1,2$, electromagnetic bands in a correlated ($r_s=2.8$) Al/Al_2O_3 superlattice ($\delta=0.721$ for $\omega_p=15$ eV, $d_{Al}=50$ Å, $d_{oxide}=500$ Å) calculated from Eq. (3.1) at $kd=0$. Compare with Fig. 3 and note that the gaps are proportional to $\sqrt{\delta}$.

lower subbands:

$$\omega_l^2(k,q)=\begin{cases} Q^2c_s^2+k^2c_s^2, & qd=0 \\ (Q-q)^2c_s^2+k^2c_s^2+\omega_p^2\alpha_-(k,q), & 0<qd<\pi \\ \left(Q-\dfrac{\pi}{d}\right)^2c_s^2+k^2c_s^2+2\omega_p^2\alpha_-\left(k,\dfrac{\pi}{d}\right), & qd=\pi \end{cases} \tag{5.1}$$

upper subbands:

$$\omega_u^2(k,q)=\begin{cases} Q^2c_s^2+k^2c_s^2+2\omega_p^2\alpha_+(k,0), & qd=0 \\ (Q+q)^2c_s^2+k^2c_s^2+\omega_p^2\alpha_+(k,q), & 0<qd<\pi \\ \left(Q+\dfrac{\pi}{d}\right)^2c_s^2+k^2c_s^2, & qd=\pi, \end{cases} \tag{5.2}$$

where $\alpha_\pm(k,q)=1$ for the TE bands and

$$\alpha_\pm(k,q)=\frac{(Q\pm q)^2}{(Q\pm q)^2+k^2} \tag{5.3}$$

for the TM bands. The TE and TM dispersion curves are displayed in Figs. 3–7. The width of a gap between a lower and upper subband at $k=0$ is calculated to be $\Delta\omega(k=0,q=0)=\omega_p\sqrt{\delta/2}/(\pi s)$. The gap width $\Delta\omega(k=0,q=0)=(0.0029/s)\omega_p$ is quite small for the semiconductor superlattice with $\delta=1.64\times10^{-4}$, whereas for the metallic superlattice discussed in Sec. III, the gap width $\Delta\omega=(0.19/s)\omega_p$ for $\delta=0.72$ is substantially larger.

VI. CONCLUSIONS

In this paper we have analyzed the role of electrodynamic retardation in mode dispersion in infinite superlattices modeled as an array of regularly spaced 2D plasma layers embedded in a dielectric material. While metallic superlattices have been of interest in the present work, our main emphasis has been on correlated semiconductor superlattices. The following are the main accomplishments of this paper.

(i) We now have a precise mathematical description of the evolution of the in-phase ($qd=0$) plasmon from its embryonic TM-electromagnetic stage [Eq. (3.3a)] in the $k<\omega_p/c_s$ domain to its optical-phonon stage [Eq. (3.3b)] in the $k>\omega_p/c_s$ domain.

(ii) In addition to the numerically generated dispersion curves in Figs. 1 and 2, we have established approximate analytical formulas for the evolution of the gapped plasmon and shear excitations from the propagating region $0\leqslant k<\omega/c_s$ to the nonpropagating region $k>\omega/c_s$ of the ωk plane. In the random-phase approximation (RPA) the in-phase plasmon and long-wavelength acoustic band lie entirely in the lower-right quadrant (of the ω, k plane) bounded by dispersion curves (3.3a,b) with $J^L_{|m|0}=0$, $K_{|m|0}=0$, $m=0,\pm1,\pm2,\ldots$); in the RPA the out-of-phase mode lies at the bottom of the acoustic band.[4] If intralayer correlations are introduced, the band of correlation-softened acoustic plasmons continues to remain confined to the lower-right quadrant again with the out-of-phase mode lying at the bot-

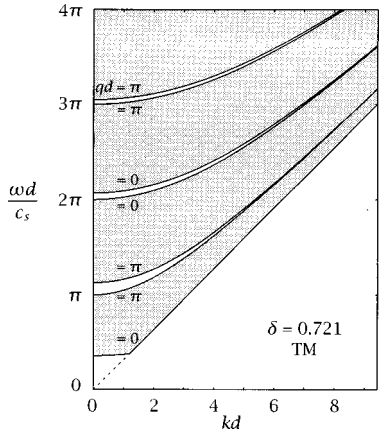

FIG. 5. Dispersion curves for the TM $s=0,1$ bands and $s=2$ lower subband in the correlated Al/Al_2O_3 ($\delta=0.721$) superlattice calculated from Eq. (3.1). Each shaded region represents a band of modes; only the in-phase ($qd=0$) and out-of-phase ($qd=\pi$) boundaries are labeled.

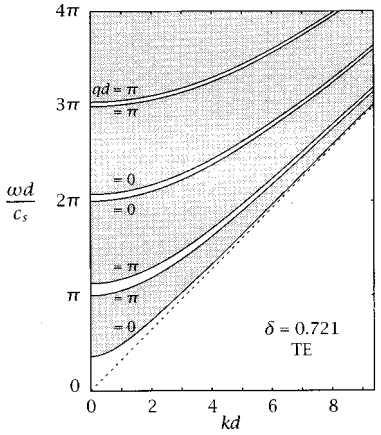

FIG. 6. Dispersion curves for the TE $s=0,1$ bands and $s=2$ lower subband in the correlated Al/Al_2O_3 ($\delta=0.721$) superlattice calculated from Eq. (4.1). Note that the narrowing of the gaps with increasing kd is a finite-δ effect not reflected in Eqs. (5.1) and (5.2).

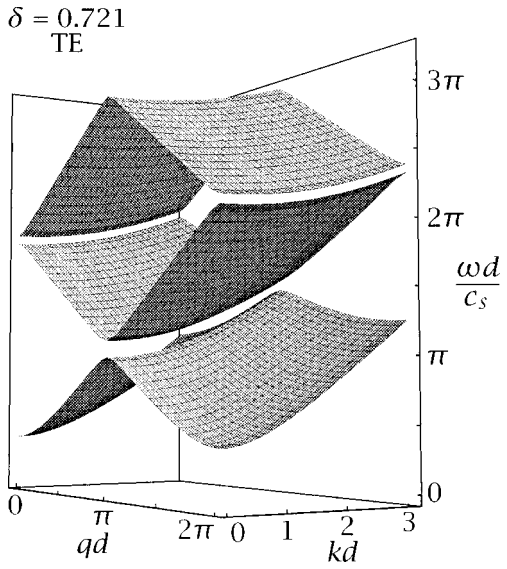

FIG. 7. Three-dimensional view of the $s=0,1$ TE electromagnetic bands for the correlated Al/Al_2O_3 ($\delta=0.721$) superlattice calculated from Eq. (4.1).

tom of the band. If interlayer correlations are also introduced, the dispersion changes dramatically with the appearance of the q-dependent energy gaps at $k=0$: the gapped plasmon band now occupies both lower quadrants bounded by dispersion curves (3.2a) and (3.3b) and at long wavelengths the out-of-phase plasmon now lies at the top of the gapped band (Fig. 1).

(iii) We have derived an approximate analytical formula [Eq. (3.2a)] for the shift in the bulk plasma frequency ω_p arising from electrodynamic retardation. This effect can be quite pronounced in metallic superlattices.

(iv) The solution (4.5) of TM Eq. (3.1) or of TE Eq. (4.1) for $(qc_s)^2 \ll \omega_p^2$ and $k=0$ depicts the shear excitation in a quadratic ($\omega \propto q^2$) stage. This excitation arises from the combined effect of strong interlayer correlations and electrodynamic retardation. The quasilocalization hypothesis underlying the derivation of Eq. (4.5) for $\omega_-(0,q)$ suggests that such an ultralow frequency wave can propagate in a semiconductor superlattice when its lattice planes are in a 2D Wigner crystal phase. For $0<kd\ll\sqrt{2\delta}$, we observe that the $\omega_-^2(0,q)$ term shows up quite naturally as the first vestige of the energy gap in the initial TM electromagnetic stage (3.6) of the plasmon.

(v) The in-phase shear excitation also has a similarly structured initial quadratic stage ($\omega \propto k^2$) arising from the same effects.

(vi) We have calculated the mode frequencies [Eqs. (5.1)–(5.3)] and dispersion curves (Figs. 3–7) for the infinite sequences of TM- and TE-polarized electromagnetic bands in an infinite superlattice of 2D plasma layers embedded in a dielectric substrate. The bands are separated by gaps that arise from the presence of the plasma layers. The analytical mode frequency formulas constitute the principal contribution to the literature[3,5] on these higher lying EM bands.

ACKNOWLEDGMENTS

This work was partially supported by NSF Grant Nos. PHY-9115615 and PHY-9115714.

*Present address: IBM Corporation, 1000 River Road, Essex Junction, VT 05452.

[1] A. Tselis, G. Gonzalez de la Cruz, and J. J. Quinn, Solid State Commun. **47**, 43 (1983); A. C. Tselis and J. J. Quinn, Phys. Rev. B **29**, 2021 (1984).

[2] Dengping Xue and Chien-hua Tsai, Solid State Commun. **56**, 651 (1985).

[3] (a) N. C. Constantinou and M. G. Cottam, J. Phys. C **19**, 739 (1986); (b) M. Babiker, N. C. Constantinou, and M. G. Cottam, *ibid.* **20**, 4581 (1987); (c) **20**, 4597 (1987).

[4] R. D. King-Smith and J. C. Inkson, Phys. Rev. B **36**, 4796 (1987).

[5] R. Haupt and L. Wendler, Phys. Status Solidi B **142**, 125 (1987).

[6] (a) Dexin Lu, K. I. Golden, G. Kalman, Ph. Wyns, L. Miao, and X.-L. Shi, Phys. Rev. B **54**, 11 457 (1996); (b) K. I. Golden, G. Kalman, L. Miao, and R. R. Snapp, *ibid.* **55**, 16 349 (1997).

[7] L. Swierkowski, D. Neilson, and J. Szymanski, Phys. Rev. Lett. **67**, 240 (1991).

[8] K. I. Golden, G. Kalman, and Ph. Wyns, Phys. Rev. A **46**, 3454 (1992).

[9] K. I. Golden and G. Kalman, Phys. Lett. A **149**, 401 (1990).

[10] A. L. Fetter, Ann. Phys. (N.Y.) **88**, 1 (1974).

[11] B. Y. Jin and J. B. Ketterson, Adv. Phys. **38**, 189 (1989).

[12] K. I. Golden, G. Kalman, and Ph. Wyns, Phys. Rev. A **46**, 3463 (1992).

[13] B. Tanatar and D. M. Ceperley, Phys. Rev. B **39**, 5005 (1989).